


Original article

Multi-factorial predictive model linking acoustic characteristics with geotechnical parameters in deep-water shallow formations

Lei Li¹, Huanhuan Wang²^{*}, Youhong Sun², Jin Yang¹, Dongyufu Zhang³, Mingxuan Hao⁴

¹College of Safety and Ocean Engineering, China University of Petroleum, Beijing 102249, P. R. China

²School of Engineering and Technology, China University of Geosciences, Beijing 100083, P. R. China

³Research Institute of Petroleum Exploration and Development (RIPED), PetroChina, Beijing 100089, P. R. China

⁴Department of Marine Technology, Norwegian University of Science and Technology, Trondheim 7052, Norway

Keywords:

Acoustic characteristics
engineering parameters
shallow sediments
relationship equations
deep-water

Cited as:

Li, L., Wang, H., Sun, Y., Yang, J., Zhang, D., Hao, M. Multi-factorial predictive model linking acoustic characteristics with geotechnical parameters in deep-water shallow formations. *Advances in Geo-Energy Research*, 2025, 18(3): 257-271.
<https://doi.org/10.46690/ager.2025.12.05>

Abstract:

Offshore infrastructure stability is controlled by deep-water shallow sediments, and the geotechnical-acoustic correlation between the two enables geological property prediction from acoustic waves. However, existing models often rely on limited sediment types or regional data, constraining their generalizability across a range of marine environments. This study presents a novel predictive model that uses a theoretical framework extending Biot's theory to integrate key geotechnical properties-clay content, density, water content, and shear strength-with acoustic parameters. By establishing the theoretical relationship between sediment parameters and acoustic responses, P-wave velocity and attenuation coefficients are computed under a range of conditions. Single-factor predictive models for each geotechnical property are derived through numerical fitting and rigorously validated against experimental data. These individual models are subsequently integrated into a comprehensive multi-factor model using multiple linear regression. Analysis of variance and Spearman's correlation analysis statistically confirm that these four parameters exert a significant and substantial influence on acoustic wave behavior. The capability of the model to simultaneously invert for multiple geotechnical properties from acoustic datasets makes it a practical tool for pre-drilling sediment characterization, enabling a more reliable, non-invasive method for site investigation that can reduce planning risks and costs. By improving the accuracy of sediment property assessment, the model contributes directly to enhanced geohazard identification and mitigation strategies, thereby promoting greater safety in the development of deep-water marine resources.

1. Introduction

Deep-water shallow sediments, defined as unconsolidated strata within 1,000 m below the mudline, consist primarily of weakly cemented silts, clays, sands, and sandy clays (Stow and Piper, 1984; Aird, 2018). These formations are characterized by high water content and plasticity compared to deeper sediments (Palix et al., 2013; Baeten et al., 2014; Wang et al., 2023b), and their engineering strength is critical for ensuring the stability of subsea infrastructure-including wellheads, conductors, pipelines, and foundations, as well as for mitigat-

ing geological hazards such as collapse and subsidence (Jin et al., 2010; Wang et al., 2022; Liao et al., 2023). The accurate prediction of their geotechnical properties relies on two main approaches: Direct measurement via sampling or *in-situ* testing and acoustic parameter-based inversion (Schnaid, 2005; Xie et al., 2024). However, direct sampling methods have significant limitations. For instance, gravity coring is typically restricted to the upper 10-m layer below the mudline (Skinner and McCave, 2003), while the more penetrating borehole coring is costly and inevitably causes soil disturbance (Ruda, 2005),

which can compromise the accuracy of subsequent laboratory measurements. This is of critical concern when measuring sensitive properties like undrained shear strength (Khadge, 2000), where different testing methods on samples from the same location can yield large variations in the results, such as in the Gulf of Mexico (Francisca et al., 2005). Despite the value of core data in establishing initial correlations, the inherent drawbacks of sampling highlight the need for robust acoustic inversion techniques (Horne, 2000) that can minimize reliance on extensive and potentially disturbed physical samples.

Over the recent decades, the establishment of acoustic-geotechnical relationships has motivated the development of numerous empirical correlations, largely centered on single-parameter predictive models (Richardson et al., 1997; Stokes and Dunn, 2001). In terms of ocean exploration, as sea water has no shear elasticity, shear waves cannot propagate in sea water and only longitudinal waves can be used to detect the shallow soil properties of the seabed (Chen et al., 2015). The acoustic characteristics in this study refer to the characteristics of acoustic longitudinal waves. A clear relationship between the acoustic characteristics and sediment properties has been established, creating a basis for this indirect approach. Initial research successfully demonstrated that key sediment properties, such as clay content or porosity (Anderson, 1974), could be empirically linked to acoustic velocity. Subsequent studies expanded this line of inquiry into diverse environments, ranging from carbonate terrains to siliciclastic shelves (Vieira et al., 2019). Multi-regression techniques had been employed to predict parameters like porosity, density, and grain size from acoustic data (Endler et al., 2015; Meng et al., 2018; Wang et al., 2023a). Although this extensive body of empirical work has firmly validated the acoustic-proxy concept, a significant limitation persists: The derived formulas are often highly specific to their source region and sediment type. This context-dependency restricts the broader applicability of these techniques, underscoring a clear need for a generalized theoretical framework that can transcend localized empirical fittings.

Building upon the recognition that acoustic characteristics are governed by the combined effect of multiple sediment properties rather than single factors, research has progressively shifted from region-specific single-parameter models (Clarke, 1994) toward multi-parameter relationships (Xu et al., 2025) grounded in theoretical frameworks. Early empirical work in various marine settings confirmed that the acoustic properties can be quantitatively linked to several geotechnical parameters, such as porosity (Liu et al., 2013), density (Uyanik et al., 2019), and mean grain size (Hansuld et al., 2012) through multivariate regressions. More recently, studies have sought to integrate theoretical models with experimental data to enhance the predictive accuracy and mechanistic insights, such as by coupling imaging techniques (Chen et al., 2023) with wave theory to estimate elastic moduli (Izotova et al., 2020) or using wave velocity to assess sediment strength indices (Xia et al., 2022; Khajevand, 2023; Zhu et al., 2024). However, most models remain largely empirical and fail to adequately account for the combined influence of key geotechnical parameters (e.g., clay content, density, water content, shear strength) on both acoustic velocity and

attenuation (Kumar et al., 2020). Given the complex interplay (Jaber, 2022; Ali et al., 2024) among these variables, studies dedicated to multi-parameter fitting formulations, particularly those simultaneously addressing velocity and attenuation, remain notably scarce. Consequently, further investigations are essential to establish a generalized quantitative relationship between acoustic and geotechnical properties in deep-water shallow sediments.

Based on Biot's theory for porous media, this study develops a theoretical framework that connects acoustic properties with key geotechnical parameters in deep-water shallow sediments. Wave velocity and attenuation are calculated based on engineering parameters derived from Biot's equations. Single-parameter models relating acoustic characteristics to clay content, density, water content, and shear strength are established through fitting and validated via laboratory experiments. Furthermore, single-factor and Spearman's correlation analyses are employed to determine the inter-parameter relationships. Finally, the multi-factor model between the acoustic characteristics and geophysical parameters of shallow sediments in deep-water is established by using function transformation and multiple linear regression.

2. Methodology

2.1 Theory

Based on the theory shown in the Supplemental file (Appendix A), the acoustic velocity v and attenuation coefficient α can be calculated by numerous parameters of shallow sediments, encompassing particle density, porosity, wet density, particle size, and various other variables, all of which are ascertained through physical property assessments, references from scholarly works, or calculations employing empirical formulae. The detailed values for these input parameters for acoustic wave computations in shallow sediments within deep-water are presented in Table 1. Furthermore, the physical characteristics, such as particle density, pore size and porosity, have been determined based on geotechnical data collected from shallow sediments in the South China Sea. Values for the remaining parameters (e.g., particle, pore water, and frame bulk moduli, and sediment shear modulus) were first determined from established literature, then they were optimized within their predefined plausible ranges (Foti et al., 2002; Williams et al., 2002; Yoon and Lee, 2010).

To elucidate the correlation between the engineering parameters and acoustic characteristics, the relationship between engineering parameters and theory parameters outlined in Table 1 can be initially proposed. By substituting certain variables in Table 1 with engineering parameters, the acoustic velocity and attenuation can be calculated with different engineering parameters.

2.1.1 Relationship between clay content and theory parameters

Shallow sediments in deep-water regions predominantly comprise silty clay. To investigate the correlation between the individual clay content and acoustic properties, it is essential to maintain a consistent density and water content. Consequently,

Table 1. Input parameters of the Biot-Stoll model for deep-water shallow formations.

Input parameter	Value
Density of grain (kg/m ³)	Obtained by measuring
Density of fluid (kg/m ³)	1,023
Porosity (-)	0.25-0.80
Grain bulk modulus (Pa)	14.70 × 10 ⁹
Modulus of pore fluid (Pa)	2.25 × 10 ⁹
Real part of frame bulk modulus (Pa)	3.70 × 10 ⁷
Real part of frame shear modulus (Pa)	2.22 × 10 ⁷
Viscosity coefficient (Pa·s)	0.001
Permeability (m ²)	1.0-10 ⁻¹¹
Tortuosity (-)	1.25
Particle size (mm)	Obtained by measuring

any variations in clay content will inevitably lead to changes in the porosity of shallow sediments.

Under the condition of constant water content, the mathematical relationship between porosity and clay content can be articulated as follows, and the derivation process of the formula is provided in the Supplemental file (Appendix B):

$$\phi = 1 - \frac{\rho(1-c)}{\rho_s(1+\varpi)} - \frac{\rho_c}{\rho_c(1+\varpi)} \quad (1)$$

where ϕ represents the porosity, ρ represents the density of sediments, c represents the clay content, ρ_s represents the density of sand particles, ϖ represents water content, and ρ_c is the density of clay particles.

When the sedimentary clay content increases, several associated factors exhibit alterations, including an increase in the size of smaller particles, a reduction in pore size, and a subsequent decrease in the permeability of shallow sediments in deep-water environments (Zhang et al., 2015). On the basis of Navier-Stokes equations, Brusckke and Advani (1993) presented a mathematical analysis that integrates the Lubrication model and Cell model to establish a correlation between permeability and porosity within porous media featuring a circular particle framework. In this context, our analysis assumes homogeneity in the size of both sand and clay particles, allowing us to articulate the relationship between clay content and the permeability of shallow sediments in deep-water (Brusckke and Advani, 1993):

$$\frac{K}{M_z^2} = \lambda_1 \frac{K_l}{M_z^2} + \lambda_2 \frac{K_c}{M_z^2} \quad (2)$$

where

$$M_z = cd_c + (1-c)d_s \quad (3)$$

$$\lambda_1 = 1 - e^{0.8\phi(\phi-1)} \quad (4)$$

$$\lambda_2 = 1 - e^{\frac{0.8\phi}{\phi-1}} \quad (5)$$

where K represents permeability, K_l and K_c are the permeability values under the Lubrication model and Cell model,

respectively, M_z denotes the average radius of soil particles, d_c and d_s are the particle sizes of clay and sand, respectively, and λ_1 and λ_2 are the two characteristic coefficients.

Utilizing the above formula, as opposed to employing the parameter configurations delineated in Table 1, the acoustic characteristics can be calculated according to the clay content. The present study employs the mathematical computation software Matlab to ascertain both acoustic velocity and acoustic attenuation. Through the scrutiny and synthesis of authentic data pertaining to deep-water shallow formations in the South China Sea, it has been observed that the clay content predominantly ranges from 0.25 to 0.75. Consequently, for the purposes of this investigation, the extremities of clay content are postulated to be 0.8 and 0.2, with a fixed water content of 0.5 and a density value of 1.75 g/cm³.

2.1.2 Relationship between density and theory parameters

Density exhibits an intricate interdependence with particle size, pore volume, and pore fluid composition. Therefore, when the clay content and water content remain unaltered, any variations in density invariably influence the porosity parameter encapsulated within the Biot-Stoll theoretical formulation. By integrating Eq. (1) into the corresponding parameters outlined in Table 1, the acoustic velocity and acoustic attenuation coefficients of shallow sediments were computed in deep-water settings under varying density conditions. Upon meticulous analysis and the synthesis of authentic deep-water shallow formation data collected from the South China Sea, it is evident that the density typically spans the range of 1.45 to 1.97 g/cm³. Hence, for this investigation, the upper and lower bounds for density were set as 1.4 g/cm³ and 2.1 g/cm³, respectively, while a water content of 0.5 and a clay content of 0.48 were maintained.

2.1.3 Relationship between water content and theory parameters

With an increase in water content, the adhesive forces between soil particles diminish, leading to a reduction in the average stress within the soil framework. This phenomenon induces the weakening of soil stiffness and triggers a corresponding decrease in the shear modulus, as reported by Wheeler et al. (2003). Furthermore, the augmentation of moisture content results in an increase in movable water content within the interstitial spaces among soil particles, accompanied by a corresponding decrease in irreducible water content. This decrease reduces the liquid meniscus curvature at the interparticle contacts, thereby diminishing the normal stress acting between the soil particles. For the studied silt-sand sediments with very low liquid limits, the increased water content leads to a looser soil fabric and a successive decline in shear modulus. Drawing upon findings from Rujikiatkamjorn et al. (2012), this relationship is defined as follows:

$$\mu_{b0} = 3.7 \times 10^6 \varpi^{-1.97} \quad (6)$$

where μ_{b0} represents the shear modulus of shallow sediments.

A meticulous examination and synthesis of empirical data on shallow formations in the deep-water regions of the South

China Sea clearly shows that the prevailing water content in such formations typically falls within the range of 0.216 to 0.875. Therefore, the upper and lower limits of water content are set as 0.2 and 0.9. Additionally, the density parameter has been consistently set at 1.75 g/cm³, while the clay content has been firmly fixed at 0.48. Instead of the corresponding parameter Settings in Table 1, Eqs. (1) and (6) were used to calculate the acoustic velocity and attenuation coefficient of shallow soil in deep-water under different water content conditions.

2.1.4 Relationship between shear strength and theory parameters

The variation in shear strength arises from changes in the soil properties. Specifically, the shear modulus and strength of water-saturated soil are primarily influenced by the pore ratio and effective consolidation pressure. Thus, a fundamental relationship exists between the shear strength and shear modulus of sediments found in shallow formations within deep-water environments. Several scholars have established empirical formulae between the shear strength and shear wave velocity through experiments and theoretical analyses (Yun et al., 2006; Moon and Ku, 2016), such as:

$$s = 5 \times 10^{-4} v_s^{2.5} \quad (7)$$

where v_s represents the shear wave velocity and s is the shear strength of the sediment. According to the principle of soil dynamics, the relationship between the shear modulus and shear wave velocity is expressed as:

$$\mu_{b0} = \rho v_s^2 \quad (8)$$

By applying Eqs. (7) and (8) simultaneously, the relationship between the real part of the shear modulus and the shear strength can be written as:

$$\mu_{b0} = 437 \rho s^{0.8} \quad (9)$$

The equation derived herein exhibits a notable similarity with the overarching structure of the relationship between μ_{b0} and s previously established by Hara et al. (1974) and Alshameri (2022). These studies derived their respective formulations through intermediate numerical calculations or the empirical fitting of experimental data. In contrast to earlier research, the findings derived from this study place a greater emphasis on the role of density in characterizing soil behavior. Thus, the relationship utilized within this study aligns more closely with the intrinsic shear characteristics of soil, enhancing its consistency with empirical soil mechanics.

By substituting Eq. (9) into the corresponding parameter configurations as outlined in Table 1, the acoustic velocity and attenuation of deep-water shallow sediments under different shear strength conditions were calculated. A comprehensive analysis of actual stratigraphic data from deep-water shallow regions within the South China Sea indicated that the consolidated undrained shear strength consistently ranged from 12.7 to 150 kPa. Therefore, the upper and lower bounds for shear strength in this study were set as 10 and 150 kPa, respectively.

2.1.5 Single-factor geotechnical-acoustic relationships

On the basis of the calculated influence trend of each engineering parameter on the sound velocity and attenuation coefficient, four popular mathematical models were selected to simulate the relationship between each engineering parameter and acoustic characteristics. Utilizing numerical analysis methods (Montgomery et al., 2021), the Sum of Squares of Errors (SSE), the Root Mean Square Error (RMSE), the Degrees of Freedom of the Error (DFE), and the coefficient of determination (R^2) were used to evaluate the accuracy of each model fit. For each engineering parameter, upon the analysis and evaluation of the four models by the aforementioned manner, the preliminary fitting formula between the engineering parameters and acoustic characteristics can be determined as:

$$SSE = \sum (y_i - \hat{y}_i)^2 \quad (10)$$

$$RMSE = \sqrt{\frac{\sum (y_i - \hat{y}_i)^2}{n}} \quad (11)$$

$$DFE = n - p - 1 \quad (12)$$

$$R^2 = 1 - \frac{\sum (y_i - \hat{y}_i)^2}{\sum (y_i - \bar{y}_i)^2} \quad (13)$$

where \sum represents the summation symbol, indicating that the squared errors of all data points are added together, y_i represents the actual value of the i -th observation, \hat{y}_i represents the predicted value for the i -th observation generated by the model, $(y_i - \hat{y}_i)$ represents the residual for the i -th data point, which is the difference between the actual and predicted values, n denotes the total number of observations, p denotes the number of independent variables in the model, and \bar{y}_i is the mean of the observed values.

2.2 Experiment

To comprehensively investigate the factors exerting an influence upon the acoustic characteristics of deep-water shallow sediments with precision, field test data were collected and a series of laboratory simulation experiments were carried out. Based on the field measured data and the experimental results, the single factor relationship fitted by the above calculation and numerical method could be verified, and then a single factor model of each engineering parameters and acoustic characteristics could be established.

2.2.1 Parameter setting

Since it is not feasible to directly prepare soil samples with specific shear strength values, soil samples with different clay content, density and water content were first prepared, then the shear strength and acoustic characteristics of different soil samples were tested. Among them, the acoustic characteristics include acoustic velocity and attenuation coefficient. From the comprehensive analysis of the data of the shallow sediments in the deep-water sediments of the South China Sea, this study employed a systematic experimental design to investigate the individual effects of three key sediment parameters: Clay content, density, and water content. The parameters were varied in three distinct groups while keeping the other two constant: For Group 1 (Experiments 1-7), clay contents from

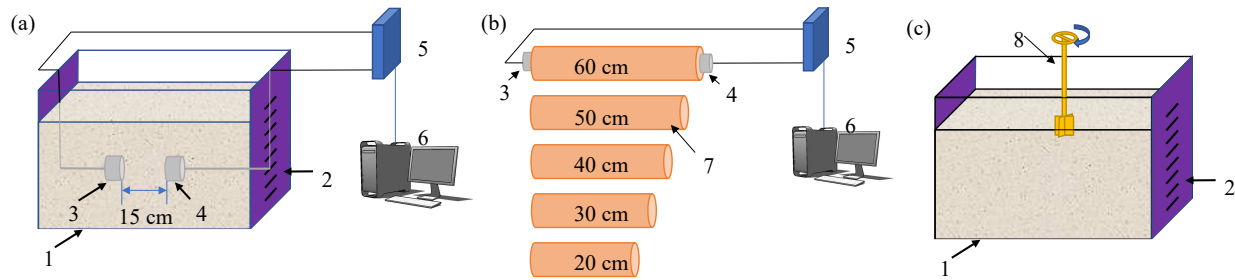


Fig. 1. Schematic of the experimental measurement system: (a) Acoustic-velocity-measuring container, (b) acoustic-attenuation-measuring container and (c) shear strength measurement method. (1: Acoustic velocity measurement of the formation vessel; 2: Sound insulation board with length scale; 3: 50-kHz acoustic transmitter; 4: Acoustic wave receiver; 5: Multi-channel data collector; 6: Data-acquisition and processing computer; 7: Formation vessel for acoustic attenuation measurement; 8: Vane Shear Tester with digital display).

0.2 to 0.8 were examined at a fixed density of 1.75 g/cm^3 and water content of 0.5. Subsequently, for Group 2 (Experiments 8-15), densities varying from 1.4 to 2.1 g/cm^3 were analyzed with constant clay content (0.48) and water content (0.5); for Group 3 (Experiments 16-23) water content from 0.2 to 0.9 was explored with constant clay content (0.48) and density (1.75 g/cm^3). This approach, encompassing a total of 23 experiments, ensured that the influence of each parameter could be isolated and accurately assessed.

2.2.2 Sample preparation

Due to the difficulty in obtaining undisturbed samples of deep-water shallow sediments, simulated soil samples with comparable physical properties were prepared using quartz sand and bentonite based on the component analysis of cuttings from a South China Sea deep-water well. The target sediments primarily consisted of quartz and clay minerals. Grain size determination was based on geotechnical data from the Ledong Formation in a deep-water well located in the Qiongdongnan Basin. The interval at 700 m below the mudline mainly comprised sand and silt, with silt particles smaller than 200 mesh. To simulate the weak cementation and high porosity of *in-situ* sediments, 80-mesh (0.115 mm) quartz sand was selected to represent the sandy fraction, while 1250-mesh bentonite was used as the clay component. Finer quartz sand was avoided to ensure that the porosity of the simulated soil matched that of the actual formation.

2.2.3 Experimental apparatus

The experimental setup (Fig. 1) enabled the simultaneous measurement of acoustic velocity, attenuation coefficient and shear strength within a simulated formation vessel, utilizing integrated acoustic transducers, a shear strength tester and a data acquisition system.

Acoustic velocity was determined by the transmission method using a “sonic detector”. Acoustic transceivers were horizontally arranged at fixed distances: 15 cm for velocity measurement and 20-60 cm for attenuation assessment. An acoustic digital instrument was used to trigger the wave, record the P-wave arrival time, and compute the velocity. Acoustic attenuation was measured using the coaxial gap attenuation

method (Hou et al., 2015). Transducers with matching frequencies were aligned horizontally and co-axially at varying distances. This configuration minimizes energy loss at the sediment-transducer interfaces, thereby reducing measurement error. Shear strength was measured with a portable digital Vane Shear Tester. Its metal disc with radial blades was inserted into the sediment and rotated at an increasing rate until shear failure occurred. The resulting torsion force was monitored to quantify the shear strength.

2.2.4 Acoustic data processing

After measuring P-wave propagation in the simulated sediments, the acoustic velocity and attenuation coefficient were calculated. Accurate velocity determination relies on the precise identification of the first arrival wave. The arrival time was measured as the interval between signal emission and this waveform discontinuity. To minimize errors from manual time reading and accurately determine the first arrival time, a wavelet analysis method was introduced, thus improving velocity calculation accuracy. Details of this method are provided in the Supplemental file (Appendix C).

The acoustic attenuation coefficient was calculated in accordance with China’s National Standard GB/T 12763.5-2007 based on the acoustic signal amplitude measured at two discrete distances. The formulation for calculating the acoustic attenuation coefficient is articulated as follows:

$$\alpha = \frac{20 \log \frac{A_2}{A_1}}{L_2 - L_1} \quad (14)$$

where α represents the acoustic attenuation coefficient, A_1 is the acoustic pressure amplitude measured at a fixed distance L_1 , and A_2 denotes the acoustic pressure amplitude measured at a fixed distance L_2 .

Following the experimental parameters, 23 sediment samples were prepared. Acoustic data were collected from seven independent measurements for each sample. To improve statistical reliability, the average value of these measurements was used to validate the theoretical models. Single-factor models were established by fitting modified formulas to relate each engineering parameter to the acoustic properties.

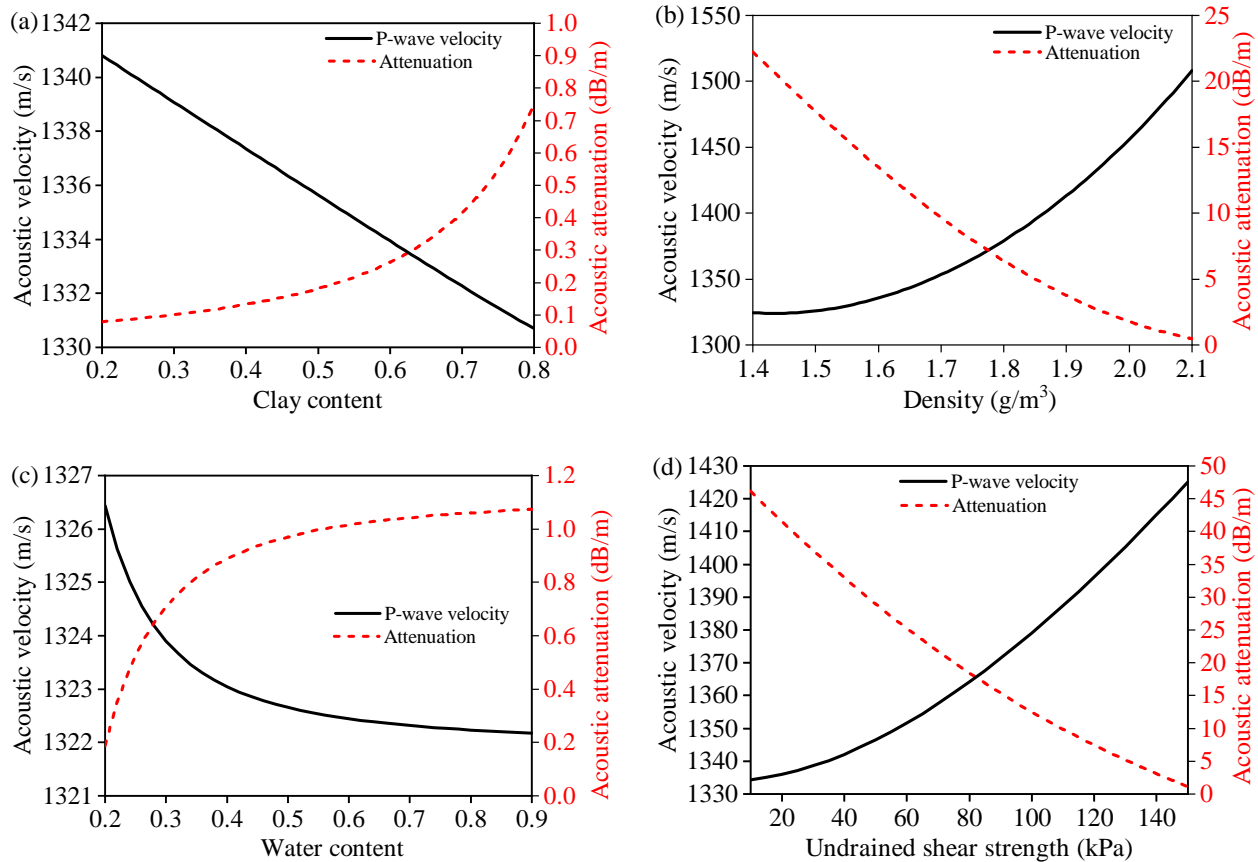


Fig. 2. Calculation results of acoustic properties with different engineering parameters: (a) clay content, (b) density, (c) water content and (d) shear strength.

2.3 Established multi-factor model

Previous analyses developed single-factor models to describe the influence of clay content, water content, density, and shear strength on acoustic properties. However, these parameters are interrelated and collectively affect acoustic behavior, necessitating the construction of a multi-factor model. This study established such a model in three steps:

1) Comparing parameter influence

ANOVA was applied to evaluate the relative impact of each parameter on the acoustic characteristics (see Appendix D in the Supplemental file).

2) Correlation analysis

Since variables are continuous but not normally distributed and may exhibit nonlinearity, Spearman correlation coefficients were used to quantify inter-parameter relationships.

3) Multi-factor model formulation

A multi-factor regression model was developed using a combined dataset of theoretical, experimental and field data. To better capture the nonlinearity, input factors were replaced with functions derived from the single-factor relationships before performing regression.

3. Results and discussion

3.1 Calculation results

Taking the theoretical calculation model presented in this paper as a basis, the calculation results of acoustic characteristics of soil layers with different clay content, density, water content, and shear strength are shown in Fig. 2. An increase in clay content correlates with a decrease in P-wave velocity and a simultaneous rise in the acoustic attenuation coefficient (Fig. 2(a)). Notably, the range of variation in acoustic velocity spans from a minimum to a maximum of 10 m/s, while the corresponding variation in acoustic attenuation encompasses a maximum-to-minimum difference of 0.65 dB/m. In light of the discerned trends governing the behavior of acoustic velocity and attenuation concerning clay content, a selection of four prevalent mathematical models, namely the polynomial model, exponential model, power function model, and logarithmic function, were employed to model the association between clay content and acoustic parameters.

Employing rigorous numerical analysis and adhering to established statistical principles, a comprehensive summary of the derived statistical insights is concisely tabulated in Table S1 in the Supplementary file (Appendix E), where several pertinent statistical metrics are presented for evaluation.

Upon analysis and evaluation of the four models, it is ascertained that the association between clay content and

acoustic velocity adheres most closely to the polynomial model. Conversely, the optimal fit for the relationship between clay content and the acoustic attenuation coefficient is found to be represented by the Exponential model. The precise mathematical formulations for these relationships are articulated as follows:

$$v = 1344 - 16.96c \quad (15)$$

$$\alpha = 0.02e^{4.39c} \quad (16)$$

The analysis of the relationship between density and acoustic properties, as shown in Fig. 2(b), indicates that an evident trend emerges where both acoustic velocity and attenuation coefficient exhibit monotonic variations with increasing density: The former demonstrates a progressive increase, while the latter shows a systematic decrease. Specifically, the P-wave velocity variation spans 190 m/s between the extreme values, accompanied by a 23 dB/m maximum differential in acoustic attenuation. Following the analytical methodology applied in the clay content study, four established mathematical models were employed to characterize these acoustic parameter variations. The corresponding statistical parameters quantifying the model fitting effectiveness are comprehensively summarized in Table S2 in the Supplementary file (Appendix E).

A systematic evaluation of the four candidate models shows that the density-acoustic velocity relationship conforms to a second-order polynomial function and the density-acoustic attenuation coefficient correlation is optimally characterized by a second-order polynomial model. These functional dependencies are mathematically formalized as:

$$v = 400\rho^2 - 1279\rho + 2247 \quad (17)$$

$$\alpha = 17.31\rho^2 - 80.21\rho + 92.28 \quad (18)$$

To quantify the acoustic response to varying water content, four established mathematical models were employed. The observed trend (Fig. 2(c)) shows a systematic decrease in P-wave velocity and a proportional increase in attenuation, with total measured variations of 4.3 m/s and 0.85 dB/m, respectively. To characterize these variations, four established mathematical models were utilized to quantify the water content-dependent acoustic responses. A quantitative comparison of model fitting performance is compiled in Table S3 in the Supplementary file (Appendix E).

A systematic evaluation of the four candidate models indicates that the water content-acoustic velocity relationship follows a power-law dependency, while the water content-acoustic attenuation coefficient correlation adheres to an exponential power-law model. The precise mathematical expressions for these relationships are delineated as follows:

$$v = 1322 + 0.16\varpi - 2.074 \quad (19)$$

$$\alpha = -0.035\varpi^{-0.2027} + 1.116 \quad (20)$$

To mathematically characterize the coupling of shear strength with the acoustic parameters, four canonical models were evaluated. The observed trends (Fig. 2(d)) show that P-wave velocity increases proportionally with shear strength, while the attenuation coefficient exhibits an inverse relationship. To mathematically characterize these dependencies,

four canonical models (polynomial, exponential, power-law, and logarithmic functions) were systematically evaluated. The quantitative metrics assessing model fidelity, including determination coefficients and root-mean-square errors, are comprehensively listed in Table S4 in the Supplementary file (Appendix E).

According to the systematic evaluation of the four candidate models, the shear strength-acoustic velocity relationship follows a power-law dependency, while the shear strength-attenuation correlation is optimally described by a second-order polynomial function. The precise mathematical formulations for these relationships are elucidated as follows:

$$v = 1333 + 0.0156s^{1.74} \quad (21)$$

$$\alpha = 0.0011s^2 - 0.4909s + 50.91 \quad (22)$$

3.2 Establishment of a single factor model

This section validates the theoretical predictions against experimental measurements to develop univariate models linking acoustic properties to geotechnical parameters in shallow sediments. The theoretical framework underwent systematic calibration through iterative comparison with empirical data, optimizing model fidelity for engineering applications.

3.2.1 Clay content

Acoustic velocity measurements from seven distinct simulated strata with varying clay contents were averaged and cross-validated against field observations. As shown in Fig. 3, the theoretical predictions calculated using Eqs. (15) and (16) demonstrate strong concordance with the experimental results. This is consistent with established empirical relationships (Buchan et al., 1972; Stokes and Dunn, 2001), though the derived slope differs regionally due to sediment composition variability. The observed correlation arises from two coupled mechanisms: (1) Increased clay content enhances sediment porosity through clay micropore proliferation, directly reducing acoustic velocity; (2) Structural lattice disruption in clay-rich sediments decreases bulk modulus, thereby lowering P-wave propagation speed. Minor deviations were observed in a small number of data points, which are attributed to inconsistencies in sediment-transducer coupling. This agreement confirms the validity of the theoretical formulation, requiring only parametric optimization as follows:

$$v = 1341 - 16.17c \quad (23)$$

A comparative evaluation against conventional linear models (Hamilton, 1970; Buchan et al., 1972; Wang et al., 2023a) confirmed the superior predictive performance of our theoretical framework, which aligns more closely with the experimental measurements (Fig. 3(b)). The P-wave attenuation coefficient exhibits a two-phase clay content dependence: Gradual growth below 0.5 clay content (Phase I) followed by accelerated attenuation above this threshold (Phase II). This phase transition arises from two synergistic mechanisms: (1) At elevated clay concentrations, reduced particle size increases particle density and the contact surface area, amplifying in-

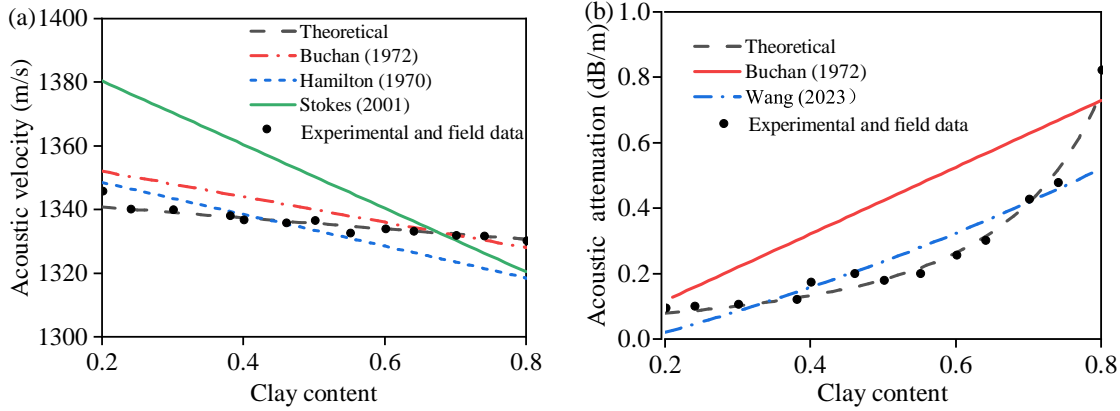


Fig. 3. Validation of the theoretical relationship between acoustic characters and clay content: (a) Acoustic velocity and (b) attenuation.

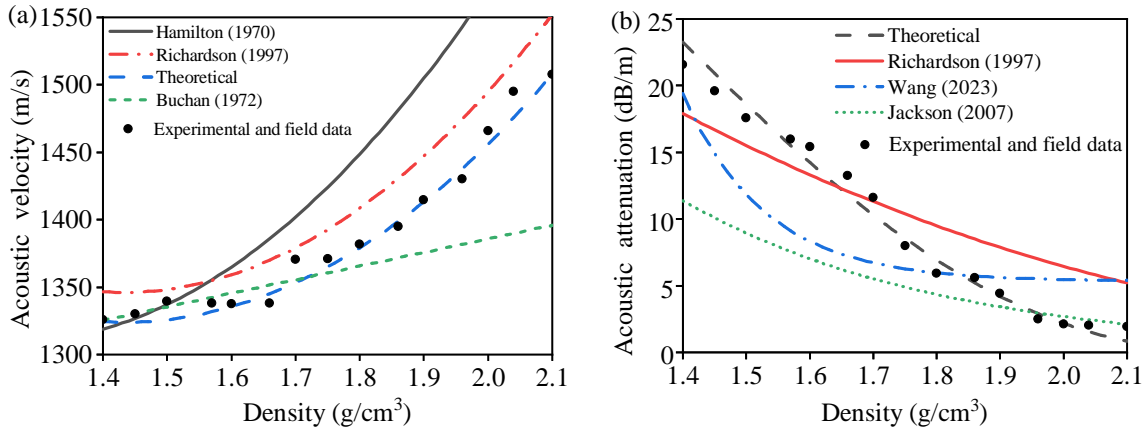


Fig. 4. Validation of the theoretical relationship between acoustic characters and density: (a) Acoustic velocity and (b) attenuation.

terparticle friction forces by 0.62-0.75 as dominant energy dissipation pathway; (2) Growing sand-clay particle size disparity generates additional heterogeneous acoustic interfaces, exacerbating reflection losses through enhanced waveform scattering and mode conversions at mineralogical boundaries.

The observed relationship between the acoustic attenuation coefficient and clay content in practical measurements closely aligns with the theoretical trend, thereby affirming the reliability and accuracy of the theoretical calculations presented in this study. Although the homogeneity of the formation is ensured as much as possible in the experiment, a full realization of uniform compaction in both the preparation of experimental sediments and the natural deposition of formations is inherently challenging. Consequently, the actual acoustic attenuation values may exceed their theoretically calculated counterparts. Taking the empirical and field-derived data as bases, it becomes evident that the theoretical formulations for acoustic attenuation as a function of clay content can benefit from minor refinements. Thus, the formulations are modified as follows:

$$\alpha = 0.019e^{0.492c} \quad (24)$$

3.2.2 Density

To validate the theoretical framework, acoustic velocity measurements from seven simulated strata with controlled density variations were averaged and integrated with field measurements. As shown in Fig. 4, theoretical predictions derived from Eqs. (17) and (18) demonstrate a consistent agreement with experimental and field observations.

A transition in the P-wave velocity trend is observed near a density of 1.7 g/cm³, marking a shift from a gradual increase to a regime of accelerated quadratic growth (Fig. 4(a)). This behavior arises from two principal mechanisms: (1) Porosity reduction enhances skeletal bulk modulus, directly amplifying P-wave propagation; (2) Nonlinear modifications to interparticle forces (Coulomb, van der Waals, and cementation effects) induce density-velocity coupling. The theoretical framework (Eq. (17)) aligns with established models (Hamilton, 1970; Buchan et al., 1972; Richardson et al., 1997) in its functional form, though regional geological variations necessitate para-

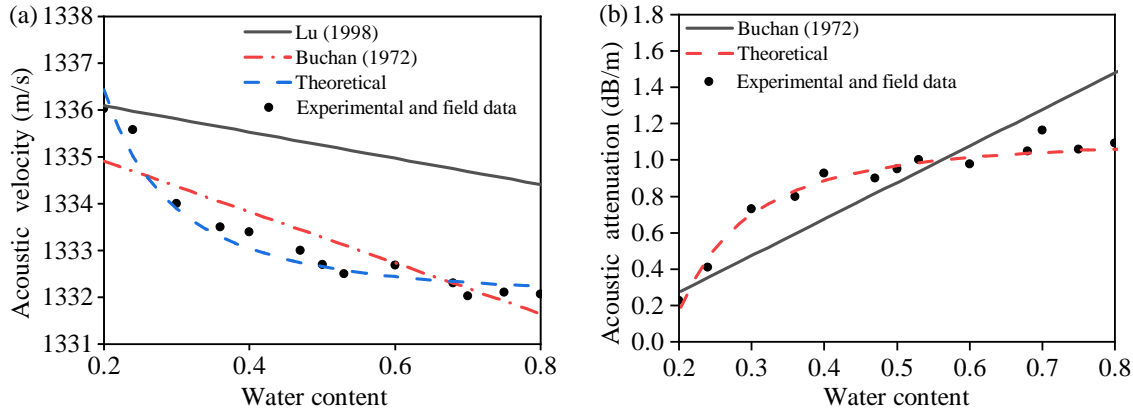


Fig. 5. Validation of the theoretical relationship between acoustic characters and water content: (a) Acoustic velocity and (b) attenuation.

metric recalibration. Experimental validation confirms that the core theoretical structure requires no substantive revision, with optimized formulations achieved through localized parameter adjustments as follows:

$$v = 400\rho^2 - 1297\rho + 2236 \quad (25)$$

Density-dependent pore size reduction in soil matrices serves as the primary mechanism governing the observed inverse correlation between density and the attenuation coefficient (Fig. 4(b)). This occurs because higher density diminishes the acoustic interfaces responsible for P-wave reflections and refractions, thereby reducing attenuation from waveform transformation. The proposed theoretical model (Eq. (18)) exhibits superior agreement with the experimental data compared to existing approaches (Richardson et al., 1997; Wang et al., 2023a). Comprehensive validation confirms that the theoretical framework requires no structural or parametric modifications, yielding the following definitive formulation:

$$\alpha = 17.31\rho^2 - 80.21\rho + 92.28 \quad (26)$$

3.2.3 Water content

The average values were computed on the basis of seven sets of acoustic characteristic data acquired from measurements conducted in simulated sediments featuring varying water content levels. Subsequently, these experimental findings were integrated with data obtained from field measurements. The comparison and analysis of the theoretical results were visually presented in Fig. 5. The theoretical acoustic velocity and attenuation results were derived from Eqs. (19) and (20), respectively. A progressive decline in P-wave velocity with increasing water content is observed, characterized by an initially rapid reduction transitioning to gradual attenuation at higher saturations (Fig. 5(a)). This behavior arises from two key mechanisms: (1) The water-induced displacement of solid particles reduces skeletal density, weakening the mechanical framework of the formation; (2) The absence of shear modulus in water diminishes the rigidity of the composite medium, directly lowering P-wave propagation efficiency. Comparative

analysis with established models (Buchan et al., 1972; Lu et al., 1998) confirms the structural validity of the theoretical framework through experimental and field validation, eliminating the requirement of parametric recalibration. The definitive water content-velocity relationship is formalized as:

$$v = 1322 + 0.16\omega^{-2.074} \quad (27)$$

The acoustic attenuation coefficient exhibits a marked augmentation with increasing water content, as illustrated in Fig. 5(b). Different from the theoretical model proposed by Buchan et al. (1972), when water content remains low, there is a pronounced acceleration in the rate of increase in the acoustic attenuation coefficient, whereas at higher water content levels, this rate of increase diminishes. This phenomenon can be attributed to the following underlying mechanism: As the water content rises, pores within the soil become saturated with water, resulting in the formation of acoustic interfaces. Consequently, P-waves undergo multiple reflections, refractions and waveform transformations at these interfaces, leading to an increase in acoustic attenuation.

The relationship observed between the acoustic attenuation coefficient and water content aligns closely with the theoretical curve derived through calculation, affirming the accuracy of the theoretical model and analytical approach proposed in this study. Notably, an anomaly is observed at a water content of 0.7, where a substantial discrepancy between experimental and theoretical data arises. However, this does not significantly impact the overall trend exhibited by the dataset. Plausible attributions for this anomaly include the potential for contact instability within the internal electrical components of the acoustic transmitting and receiving transducers under the condition of elevated water content. Upon comprehensive evaluation of the measured data in conjunction with the theoretical outcomes, it is evident that no fundamental adjustments to the form and functional type of the theoretical formula are warranted. Instead, minor parameter adjustments are deemed sufficient, yielding the following modified model:

$$\alpha = -0.035\omega^{-1.965} + 1.116 \quad (28)$$

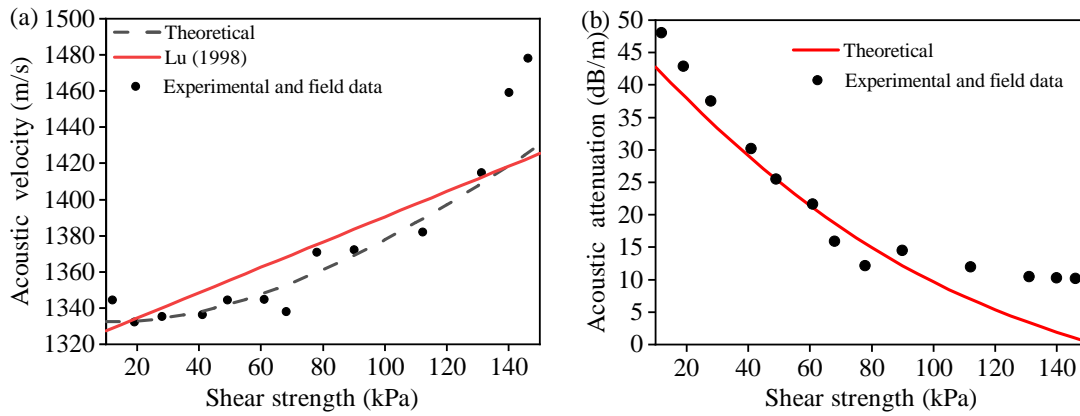


Fig. 6. Validation of the theoretical relationship between acoustic characters and shear strength: (a) Acoustic velocity and (b) attenuation.

3.2.4 Shear strength

The experimental protocol generated 23 sediment samples, each undergoing seven acoustic measurement cycles. The systematic analysis focused on 13 representative shear strength groups selected from this dataset. The acoustic velocity and attenuation coefficients were averaged across simulated formation replicates within each group, then combined with field measurements for comparative analysis against theoretical predictions (Fig. 6). The theoretical velocity and attenuation values were calculated using Eqs. (21) and (22), respectively. The dual influence of shear strength on formation properties gives rise to a nonlinear correlation with acoustic velocity (Fig. 6(a)), a relationship that contrasts with the linear model proposed by Lu et al. (1998). This behavior originates from the dual influence of shear strength on the formation properties: (1) Density enhancement through porosity reduction elevates the bulk modulus, directly amplifying acoustic wave propagation; (2) Interparticle force modifications (Coulomb, van der Waals, and cementation effects) induce nonlinear stiffness responses. Concurrently, shear modulus augmentation at higher shear strengths further accelerates acoustic velocity, particularly above 110kPa where rapid escalation occurs due to the synergistic density-stiffness coupling. Systematic validation against experimental and field measurements confirms the structural and parametric robustness of the theoretical framework. The observed congruence between empirical trends and model predictions obviates the need for functional or parametric revisions. The validated single-factor acoustic velocity-shear strength relationship is formalized as:

$$v = 1333 + 0.0156s^{1.74} \quad (29)$$

Increasing shear strength corresponds to a decrease in the acoustic attenuation coefficient, as evidenced in Fig. 6(b). This behavior arises from shear strength-induced density enhancement, which reduces sediment pore dimensions and consequently diminishes acoustic interfaces driving wave reflections, refractions, and waveform transformations. The experimental measurements exhibit good agreement with the theoretical predictions, though parametric optimization of the

theoretical framework enhances the predictive accuracy. The refined formulation is expressed as:

$$\alpha = 0.0024s^2 - 0.62s + 42 \quad (30)$$

3.3 Establishment of multi-factor model

3.3.1 Comparative influence of parameters

One-way ANOVA was performed on acoustic velocity and attenuation coefficients across four geotechnical parameters using experimental and field data. The statistical results (Tables 2 and 3) present the following key metrics: Sum of squared deviations (SS), degrees of freedom (DF), mean squares (MS), between-group to within-group variance ratio (F-statistic), probability associated with observed F-statistic (P-value), and threshold at χ confidence level for df_A and df_e degrees of freedom (F critical value).

The single-factor ANOVA analysis of clay content, water content, density, and shear strength reveals their hierarchical influence on acoustic velocity. Shear strength dominates as the primary determinant, followed sequentially by density and clay content. Although water content exhibits the weakest correlation, all four parameters demonstrate statistically significant effects ($P < 0.001$) through rigorous hypothesis testing.

Shear strength persists as the dominant determinant of acoustic attenuation coefficient variability, with density and water content exhibiting secondary influences in a decreasing order of magnitude. While clay content demonstrates the weakest correlation, all four geotechnical parameters show statistically significant effects through rigorous hypothesis testing, confirming their collective impact on the attenuation characteristics.

3.3.2 Correlation analysis

Given the non-normal distributions and nonlinear dependencies among the investigated continuous variables, Spearman's coefficient emerged as the optimal metric for assessing geotechnical-acoustic interactions. Fig. 7 presents the multivariate correlation matrix visualizing the interdependencies between acoustic velocity and key engineering parameters

Table 2. One-way ANOVA of acoustic velocity with different engineering parameters.

Parameter	Difference source	SS	DF	MS	F	P-value	F-crit
Clay content	Between groups	585.2	6	97.54	172.1	6.4×10^{-28}	2.324
	Within-group	23.81	42	0.5668	172.1	6.4×10^{-28}	2.324
	Total	609.1	48	/	/	/	/
Density	Between groups	224,529	10	22,452	202.9	5.4×10^{-38}	2.018
	Within-group	5,751	52	110.6	202.9	5.4×10^{-38}	2.018
	Total	230,281	62	/	/	/	/
Water content	Between groups	102.9	7	14.69	22.43	3.9×10^{-13}	2.207
	Within-group	31.44	48	0.6549	22.43	3.9×10^{-13}	2.207
	Total	134.3	55	/	/	/	/
Shear strength	Between groups	255,810	12	21,317	263.3	7.6×10^{-58}	1.878
	Within-group	6,315.7	78	80.97	263.3	7.6×10^{-58}	1.878
	Total	262,126	90	/	/	/	/

Table 3. One-way ANOVA of acoustic attenuation with different engineering parameters.

Parameter	Difference source	SS	DF	MS	F	P-value	F-crit
Clay content	Between groups	2.918	6	0.4863	98.81	3.8×10^{-23}	2.324
	Within-group	0.2067	42	0.0049	98.81	3.8×10^{-23}	2.324
	Total	3.124	48	/	/	/	/
Density	Between groups	11,322	10	1,132	232.28	2.2×10^{-47}	1.977
	Within-group	321.7	66	4.874	232.28	2.2×10^{-47}	1.977
	Total	11,644	76	/	/	/	/
Water content	Between groups	4.514	7	0.6449	84.98	7.6×10^{-25}	2.207
	Within-group	0.3643	48	0.00758	84.98	7.6×10^{-25}	2.207
	Total	4.878	55	/	/	/	/
Shear strength	Between groups	14,938	12	1,244	307.8	2×10^{-60}	1.878
	Within-group	315.5	78	4.04517	307.8	2×10^{-60}	1.878
	Total	15,254	90	/	/	/	/

(clay content, water content, density, shear strength). Specifically, velocity exhibits an inverse correlation with clay and water contents, consistent with the theoretical predictions of porosity-mediated wave attenuation. Conversely, positive correlations manifest with density and shear strength, reflecting bulk modulus enhancement and interparticle force optimization. All parameters demonstrate a non-negligible influence (correlation magnitude > 0.1), necessitating their inclusion in predictive regression frameworks. Critically, interparameter correlations remain subcritical (absolute values < 0.75), confirming statistical independence and precluding multicollinearity concerns in multivariate modeling.

To analyze and visualize the correlation between the acous-

tic attenuation coefficient and the engineering parameters, namely clay content, water content, density, and shear strength, this study utilized the Spearman correlation coefficient matrix. The results of this analysis are presented in Fig. 8. The acoustic attenuation coefficient exhibits distinct positive correlations with clay and water contents, aligning with the theoretical models of porosity-driven scattering and fluid-solid interaction losses. Conversely, inverse relationships manifest with density and shear strength, reflecting pore reduction and interparticle contact optimization. All parameters exhibit a non-negligible influence, necessitating their inclusion in predictive frameworks. Critically, interparameter correlations remain subcritical, confirming statistical independence and precluding multi-

Table 4. Dependent variable and input feature substitution relationship of multiple regression.

Dependent variable	Independent variable	Initial input	Input after function replacement
Acoustic velocity	Clay content	x_{1t}	$x_1 = 1341 - 16.17x_{1t}$
	Density	x_{2t}	$x_2 = 400x_{2t}^2 - 1297x_{2t} + 2236$
	Water content	x_{3t}	$x_3 = 1322 + 0.16x_{3t}^{-2.074}$
	Shear strength	x_{4t}	$x_4 = 1333 + 0.0156x_{4t}^{1.74}$
Acoustic attenuation	Clay content	x_{1t}	$x_1 = 0.019e^{4.92x_{1t}}$
	Density	x_{2t}	$x_2 = 17.31x_{2t}^2 - 80.21x_{2t} + 92.28$
	Water content	x_{3t}	$x_3 = -0.035x_{3t}^{-1.965} + 1.116$
	Shear strength	x_{4t}	$x_4 = 0.0024x_{4t}^2 - 0.62x_{4t} + 42$

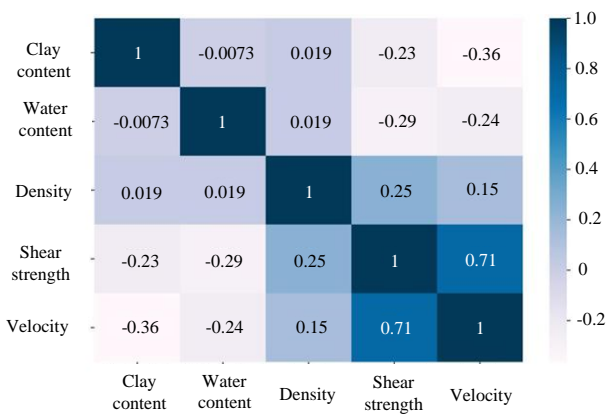


Fig. 7. Correlation matrix of acoustic velocity and four factors.

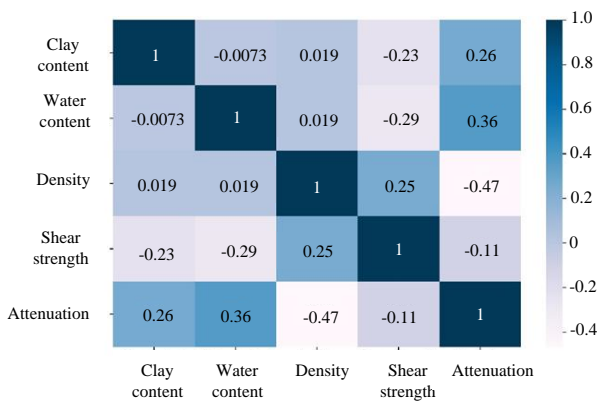


Fig. 8. Correlation matrix of acoustic attenuation and four factors.

icollinearity concerns in multivariate regression modeling.

3.3.3 Multi-factor model of acoustic characteristics

This study integrates theoretical, experimental and field-derived data to develop multi-factorial equations for acoustic velocity and the attenuation coefficient through multivariate regression analysis. Correlation analysis identifies clay content, water content, density, and shear strength as essential predictors for both acoustic parameters, with identical variable

sets selected to ensure model symmetry and comparative consistency.

The multivariate regression framework, comprising four independent variables and one dependent parameter, necessitates nonlinear parameterization to address inherent nonlinear dependencies between geotechnical factors and acoustic properties. Given these nonlinear interactions, traditional linear regression assumptions prove inadequate. To enhance model fidelity, functional substitutions of input variables, derived from single-factor relationships (Table 4), are incorporated using an enhanced algorithm. This transformation yields updated formulations for both acoustic velocity (Eq. (32)) and attenuation (Eq. (34)), derived from their initial multivariate expressions (Eqs. (31) and (33)), while preserving physical interpretability:

$$v = \beta_0 + \beta_1 x_1 + \beta_2 x_2 + \beta_3 x_3 + \beta_4 x_4 \quad (31)$$

$$v = \beta_0 + \beta_1 (1341 - 16.17x_{1i}) + \beta_2 (400x_{2i}^2 - 1297x_{2i} + 2236) + \beta_3 (1322 + 0.16x_{3i}^{-2.074}) + \beta_4 (1333 + 0.0156x_{4i}^{1.74}) \quad (32)$$

$$\alpha = \beta_0 + \beta_1 x_1 + \beta_2 x_2 + \beta_3 x_3 + \beta_4 x_4 \quad (33)$$

$$\alpha = \beta_0 + \beta_1 (0.019e^{4.92x_{1i}}) + \beta_2 (17.31x_{2i}^2 - 80.21x_{2i} + 92.28) + \beta_3 (-0.035x_{3i}^{-1.965} + 1.116) + \beta_4 (0.0024x_{4i}^2 - 0.62x_{4i} + 42) \quad (34)$$

where β_0 , β_1 , β_2 , β_3 , and β_4 are the coefficients to be determined by the regression analysis.

By integrating theoretical, experimental and field data, the multi-factorial acoustic model was analyzed through multivariate linear regression with functional parameterization. The derived acoustic velocity formulation is formalized as:

$$v = 1962.09 + 0.93c + 266\rho^2 - 862.5\rho + 151.58\varpi^{-2.074} + 0.0189s^{1.74} \quad (35)$$

The inclusion of the ρ^2 term is not merely a statistical art-

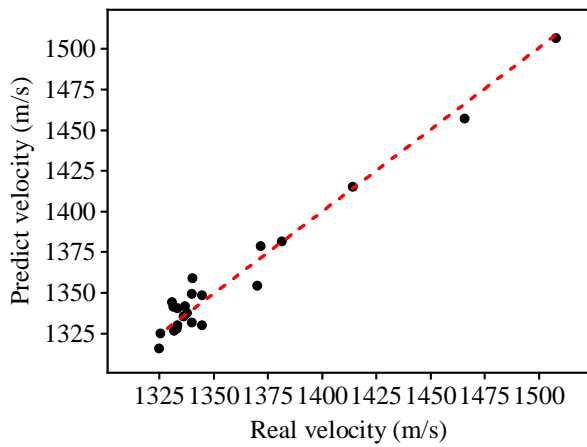


Fig. 9. Crossplot of predicted and measured acoustic velocities.

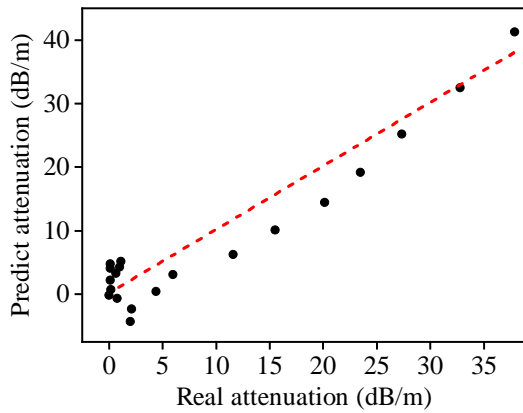


Fig. 10. Crossplot of predicted and measured acoustic attenuation coefficient.

ifact but is intended to capture the non-linear effects of sediment compaction and grain-to-grain contact stiffness. At higher densities (greater compaction), the increase in acoustic velocity is nonlinear because the sediment frame becomes significantly stiffer. Shear strength is a direct macroscopic measure of the shear modulus and cohesion of the sediment frame. It quantifies the ability of the skeletal frame to sustain shear stresses, which is critical for the propagation of shear waves and significantly influences the compression wave velocity through frame elasticity: A stronger frame reduces energy loss due to irreversible grain sliding and friction.

This study evaluates multivariate regression models using two key metrics: RMSE and R^2 . The established acoustic velocity multi-factor model demonstrates an excellent goodness of fit, with an R^2 of 0.9691. Fig. 9 shows a strong agreement between the predicted and measured acoustic velocities. These results confirm the high predictive accuracy and robust data fidelity of the multivariate regression model.

Similarly, the multi-factor regression model of acoustic attenuation coefficient is obtained as:

$$\alpha = 171.18 + 0.00019e^{4.72c} + 33.93\rho^2 - 157.21\rho - 211.33\varpi^{-1.965} - 0.00047s^2 + 0.1207s - 8.17 \quad (36)$$

Parameters like clay content and water content are directly linked to viscous dissipation. Clay content affects pore fluid viscosity and the specific surface area for fluid-particle interaction, while water content defines the volume of the viscous fluid. Together, these parameters control the Biot-type viscous damping as the pore fluid moves relative to the solid skeleton under acoustic excitation. The predictive performance of the acoustic attenuation model is demonstrated in Fig. 10, showing strong agreement between theoretical predictions and experimental measurements. Combined analysis of the correlation plot and evaluation metrics (RMSE = 3.77, $R^2 = 0.8863$) validates the robust predictive capability and strong empirical concordance of the multivariate acoustic attenuation model.

4. Conclusions

This study established predictive models for the acoustic properties of deep-water shallow sediments by integrating Biot's theory with theoretical calculations, laboratory simulations, and field measurements.

The developed single-factor models revealed distinct relationships: P-wave velocity decreases linearly with clay content but increases nonlinearly with density, while the acoustic attenuation coefficient grows exponentially with clay content and decreases with increasing density. Meanwhile, water content exhibits an inverse exponential correlation with both velocity and attenuation. Shear strength critically influences both properties, accelerating P-wave velocity exponentially and reducing attenuation quadratically.

Sensitivity analysis identified shear strength and density as the dominant controlling factors, followed by clay and water contents. All four engineering parameters showed strong correlations with the acoustic properties while maintaining statistical independence. An optimized multivariate linear regression model, incorporating functionally transformed clay content, density, water content, and shear strength, have been established. This model achieves high predictive accuracy.

This model provides an innovative tool for deep-water engineering, enabling the precise prediction of shear strength via acoustic parameter inversion. This capability significantly enhances the reliability of subsea pipeline routing and platform foundation design. As a limitation of the multi-factor model developed in this study, it does not account for interactions between parameters. Future work could incorporate such interaction terms and involve the development and validation of models for different frequency ranges and sediment types. Furthermore, the validation of both *in-situ* shallow samples and laboratory-prepared specimens in the future will enhance the reliability of the proposed method.

Acknowledgements

The authors acknowledge the financial support from the National Key Research and Development Plan of China (No. 2022YFC2806402), the Natural Science Foundation of China (Nos. U22B20126 and 52404013), and the China Postdoctoral Science Foundation (No. 2025T180800) for funding this study. This research was also supported by the Key Laboratory of Polar Geology and Marine Mineral Resources (China University

of Geosciences, Beijing), Ministry of Education (No. HNPY-202413) and the specific research fund of the Innovation Platform for Academicians of Hainan Province.

Conflict of interest

The authors declare no competing interest.

Open Access This article is distributed under the terms and conditions of the Creative Commons Attribution (CC BY-NC-ND) license, which permits unrestricted use, distribution, and reproduction in any medium, provided the original work is properly cited.

References

- Aird, P. *Deepwater Drilling: Well Planning, Design, Engineering, Operations, and Technology Application*. Gulf Professional Publishing, Houston, USA, 2018.
- Ali, M., Changxingyue, H., Wei, N., et al. Optimizing seismic-based reservoir property prediction: A synthetic data-driven approach using convolutional neural networks and transfer learning with real data integration. *Artificial Intelligence Review*, 2024, 58(1): 31.
- Alshameri, B. Prediction the shear strength and shear modulus of sand-clay mixture using bender element. *Journal of Applied Engineering Science*, 2022, 20(1): 168-176.
- Anderson, R. S. Statistical correlation of physical properties and sound velocity in sediments, in *Physics of Sound in Marine Sediments*, edited by L. Hampton, Springer, Boston, MA, pp. 157-243, 1974.
- Baeten, N. J., Laberg, J. S., Vanneste, M., et al. Origin of shallow submarine mass movements and their glide planes-sedimentological and geotechnical analyses from the continental slope off northern Norway. *Journal of Geophysical Research: Earth Surface*, 2014, 119(11): 2335-2360.
- Bruschke, M., Advani, S. Flow of generalized newtonian fluids across a periodic array of cylinders. *Journal of Rheology*, 1993, 37(3): 479-498.
- Buchan, S., McCann, D. M., Smith, D. T. Relations between the acoustic and geotechnical properties of marine sediments. *Quarterly Journal of Engineering Geology Hydrogeology*, 1972, 5(3): 265-284.
- Chen, J., Hu, G., Bu, Q., et al. Elastic wave velocity of marine sediments with free gas: Insights from ct-acoustic observation and theoretical analysis. *Marine and Petroleum Geology*, 2023, 150: 106169.
- Chen, W., Wang, Z., Zhao, K., et al. Reflection of acoustic wave from the elastic seabed with an overlying gassy poroelastic layer. *Geophysical Journal International*, 2015, 203(1): 213-227.
- Clarke, J. H. Toward remote seafloor classification using the angular response of acoustic backscattering: A case study from multiple overlapping GLORIA data. *IEEE Journal of Oceanic Engineering*, 1994, 19(1): 112-127.
- Endler, M., Endler, R., Bobertz, B., et al. Linkage between acoustic parameters and seabed sediment properties in the south-western Baltic sea. *Geo-Marine Letters*, 2015, 35(2): 145-160.
- Foti, S., Lai, C. G., Lancellotta, R. Porosity of fluid-saturated porous media from measured seismic wave velocities. *Géotechnique*, 2002, 52(5): 359-373.
- Francisca, F., Yun, T. S., Ruppel, C., et al. Geophysical and geotechnical properties of near-seafloor sediments in the northern Gulf of Mexico gas hydrate province. *Earth and Planetary Science Letters*, 2005, 237(3-4): 924-939.
- Hamilton, E. L. Sound velocity and related properties of marine sediments, North Pacific. *Journal of Geophysical Research*, 1970, 75(23): 4423-4446.
- Hansuld, E. M., Briens, L., Sayani, A., et al. An investigation of the relationship between acoustic emissions and particle size. *Powder Technology*, 2012, 219: 111-117.
- Hara, A., Ohta, T., Niwa, M., et al. Shear modulus and shear strength of cohesive soils. *Soils and Foundations*, 1974, 14(3): 1-12.
- Horne, J. K. Acoustic approaches to remote species identification: A review. *Fisheries Oceanography*, 2000, 9(4): 356-371.
- Hou, Z., Guo, C., Wang, J., et al. Seafloor sediment study from South China Sea: Acoustic & physical property relationship. *Remote Sensing*, 2015, 7(9): 11570-11585.
- Izotova, V., Petrov, D., Pankratova, K., et al. Research of acoustic characteristics and physical and mechanical properties of quaternary soils. Paper 202051130 Presented at Engineering and Mining Geophysics, Perm, Russia, 14-18 May, 2020.
- Jaber, R. Investigation of the relationships between geotechnical sediment properties and sediment dynamics using geotechnical and geophysical field measurements. Virginia, Virginia Polytechnic Institute and State University, 2022.
- Jin, Y., Shujie, L., Jianliang, Z., et al. Research of conductor setting depth using jetting in the surface of deepwater. Paper SPE 130523 Presented at SPE International Oil and Gas Conference and Exhibition in China, Beijing, China, 8-10 June, 2010.
- Khadge, N. Geotechnical properties of surface sediments in the index area. *Marine Georesources & Geotechnology*, 2000, 18(3): 251-258.
- Khajevand, R. Estimating geotechnical properties of sedimentary rocks based on physical parameters and ultrasonic P-wave velocity using statistical methods and soft computing approaches. *Iranian Journal of Science Technology, Transactions of Civil Engineering*, 2023, 47(6): 3785-3809.
- Kumar, V., Vardhan, H., Murthy, C. S. Multiple regression model for prediction of rock properties using acoustic frequency during core drilling operations. *Geomechanics and Geoengineering*, 2020, 15(4): 297-312.
- Liao, B., Wang, J., Sun, J., et al. Microscopic insights into synergism effect of different hydrate inhibitors on methane hydrate formation: Experiments and molecular dynamics simulations. *Fuel*, 2023, 340: 127488.
- Liu, B., Han, T., Kan, G., et al. Correlations between the in situ acoustic properties and geotechnical parameters of sediments in the Yellow Sea, China. *Journal of Asian Earth Sciences*, 2013, 77: 83-90.
- Lu, T., Bryant, W. R., Slowey, N. C. Regression analysis of

- physical and geotechnical properties of surface marine sediments. *Marine Georesources & Geotechnology*, 1998, 16(3): 201-220.
- Meng, Q., Liu, S., Jia, Y., et al. Analysis on acoustic velocity characteristics of sediments in the northern slope of the South China Sea. *Bulletin of Engineering Geology and the Environment*, 2018, 77(3): 923-930.
- Montgomery, D. C., Peck, E. A., Vining, G. G. *Introduction to linear regression analysis*. John Wiley & Sons, Hoboken, USA, 2021.
- Moon, S.-W., Ku, T. Empirical estimation of soil unit weight and undrained shear strength from shear wave velocity measurements. Paper Presented at 5th International Conference on Geotechnical and Geophysical Site Characterisation, Gold Coast, Australia, 5-9 September, 2016.
- Palix, E., Wu, H., Chan, N., et al. Liwan 3-1: How deepwater sediments from South China Sea compare with gulf of guinea sediments. Paper OTC 24010 Presented at Offshore Technology Conference, Houston, Texas, 6-9 May, 2013.
- Richardson, M. D., Lavoie, D. L., Briggs, K. B. Geoacoustic and physical properties of carbonate sediments of the lower florida keys. *Geo-Marine Letters*, 1997, 17(4): 316-324.
- Ruda, T., Farrar, J. Environmental drilling for soil sampling, rock coring, borehole logging, and monitoring well installation, in *Practical Handbook of Environmental Site Characterization and Ground-Water Monitoring*, edited by D. M. Nielsen, CRC Press, Boca Raton, Florida, USA, pp. 298-343, 2005.
- Rujikiatkamjorn, C., Heitor, A., Indraratna, B. The effect of dry unit weight, suction, and imparted energy on the modulus of a compacted mixture of sand and kaolin. *Advances in Transportation Geotechnics 2*, 2012, 1: 18.
- Schnaid, F. Geo-characterisation and properties of natural soils by in situ tests. Paper Presented at Proceedings of the 16th International Conference on Soil Mechanics and Geotechnical engineering, Osaka, Japan, 12-16 September, 2005.
- Skinner, L., McCave, I. Analysis and modelling of gravity-and piston coring based on soil mechanics. *Marine Geology*, 2003, 199(1-2): 181-204.
- Stokes, T. L., Dunn, D. A. Acoustic and physical property correlation of marine sediments from the texas-louisiana continental shelf. Paper MTS 0-933957-28-9 Presented at MTS/IEEE Oceans 2001, Honolulu, HI, USA, 5-8 November, 2001.
- Stow, D., Piper, D. Deep-water fine-grained sediments: Facies models. Geological Society, London, Special Publications, 1984, 15(1): 611-646.
- Uyanik, O., Sabbağ, N., Uyanik, N. A., et al. Prediction of mechanical and physical properties of some sedimentary rocks from ultrasonic velocities. *Bulletin of Engineering Geology and the Environment*, 2019, 78(8): 6003-6016.
- Vieira, F. V., Bastos, A. C., Quaresma, V. S., et al. Along-shelf changes in mixed carbonate-siliciclastic sedimentation patterns. *Continental Shelf Research*, 2019, 187: 103964.
- Wang, H., Yang, J., Zhang, D., et al. Experimental study of drilling riser and wellhead force by small scale testing. *Ocean Engineering*, 2022, 256: 111489.
- Wang, J., Kan, G., Li, G., et al. Physical properties and in situ geoacoustic properties of seafloor surface sediments in the East China Sea. *Frontiers in Marine Science*, 2023a, 10: 1195651.
- Wang, Y., Zhang, S., Ren, Y., et al. Characterization of engineering properties of deep-water soils in the South China Sea. *Engineering Geology*, 2023b, 320: 107138.
- Wheeler, S. J., Sharma, R. S., Buisson, M. S. R. Coupling of hydraulic hysteresis and stress-strain behaviour in unsaturated soils. *Géotechnique*, 2003, 53(1): 41-54.
- Williams, K. L., Jackson, D. R., Thorsos, E. I., et al. Comparison of sound speed and attenuation measured in a sandy sediment to predictions based on the biot theory of porous media. *IEEE Journal of Oceanic Engineering*, 2002, 27(3): 413-428.
- Xia, K., Chen, C., Wang, T., et al. Estimating the geological strength index and disturbance factor in the hoek-brown criterion using the acoustic wave velocity in the rock mass. *Engineering Geology*, 2022, 306: 106745.
- Xie, H., Gao, M., Zhang, R., et al. Application prospects of deep *in-situ* condition-preserved coring and testing systems. *Advances in Geo-Energy Research*, 2024, 14(1): 12-24.
- Xu, S., Liu, Y., Zou, Z., et al. Boreholefull-waveform inversion of monopolelogging in slow formations: Insights for shear-wave velocity profiling. *Advances in Geo-Energy Research*, 2025, 17(1): 82-90.
- Yoon, H.-K., Lee, J.-S. Field velocity resistivity probe for estimating stiffness and void ratio. *Soil Dynamics and Earthquake Engineering*, 2010, 30(12): 1540-1549.
- Yun, T. S., Narsilio, G. A., Santamarina, J. C. Physical characterization of core samples recovered from Gulf of Mexico. *Marine and Petroleum Geology*, 2006, 23(9-10): 893-900.
- Zhang, M., Zhu, X., Yu, G., et al. Permeability of muddy clay and settlement simulation. *Ocean Engineering*, 2015, 104: 521-529.
- Zhu, Y., Yang, X., Huang, X., et al. Acoustic characterization of hydrate formation and decomposition in clay-bearing sediments. *Petroleum Science*, 2024, 21(4): 2830-2838.